Bioorganic & Medicinal Chemistry 20 (2012) 2540–2548

Contents lists available at SciVerse ScienceDirect

Bioorganic & Medicinal Chemistry

journal homepage: www.elsevier.com/locate/bmc

Synthesis and biological evaluation of bifendate–chalcone hybrids as a new class of potential P-glycoprotein inhibitors

Xiaoke Gu [a,b], Zhiguang Ren [c,d], Xiaobo Tang [a,b], Hui Peng [c,*], Yuanfang Ma [d], Yisheng Lai [a,b], Sixun Peng [a,b], Yihua Zhang [a,b,*]

[a] State Key Laboratory of Natural Medicines, China Pharmaceutical University, Nanjing 210009, PR China
[b] Center of Drug Discovery, China Pharmaceutical University, Nanjing 210009, PR China
[c] Department of Molecular Immunology, Institute of Basic Medical Sciences, Beijing 100850, PR China
[d] Institute of Immunology, Medical School of Henan University, Kaifeng 475001, PR China

ARTICLE INFO

Article history:
Received 15 January 2012
Revised 21 February 2012
Accepted 22 February 2012
Available online 3 March 2012

Keywords:
P-gp inhibitor
Bifendate
Chalcone
Multidrug resistance
Cancer chemotherapy

ABSTRACT

Overexpression of P-glycoprotein (P-gp) is one of the major problems to successful cancer chemotherapy. To find novel effective P-gp inhibitors, a series of bifendate–chalcone hybrids were synthesized and evaluated. Among them, the most active compound **8g** had little intrinsic cytotoxicity (IC_{50} > 200 μM), and could increase accumulation of Rhodamine 123 in K562/A02 cells more potently than bifendate and verapamil (VRP) by inhibiting P-gp efflux function. And **8g** displayed potent chemo-sensitizing effect and persisted for much longer time (>24 h) compared with VRP (<6 h). In addition, **8g**, unlike VRP, showed no stimulation on the P-gp ATPase activity, suggesting it is not a P-gp substrate. Therefore, **8g** may represent a promising lead to develop MDR reversal agents for cancer chemotherapy.

1. Introduction

Multidrug resistance (MDR) is regarded as a leading cause for failure of cancer chemotherapy.[1] The mechanisms underlying MDR are complicated, one of them is the overexpression of P-glycoprotein (P-gp, MDR1/ABCB1), a member of ATP-binding cassette (ABC) transporter superfamily, which pumps antineoplastic drugs out of the tumor cells, lowering intracellular drug levels, and consequently leading to drug insensitivity.[2] Coadministration of the anticancer drugs with a P-gp inhibitor is considered to be an attractive approach to overcome P-gp-mediated MDR.[3] Indeed, during past decades a large amount of compounds have been evaluated as P-gp inhibitors, including the third generation inhibitors zosuquidar, tariquidar and elacridar. Although they have showed potent P-gp inhibitory effects in animals, their clinical efficacy is disappointing for many reasons, such as low selectivity, poor \potency, inherent toxicity and/or adverse pharmacokinetic interaction with anticancer drugs.[4] So far, no drugs of this class have entered market, therefore, there is an unmet requirement for developing novel effective P-gp inhibitors.[5] Presently, researchers have turned to natural products and their synthetic derivatives, which are inhibitors of one or more ABC drug efflux pumps, and usually low in toxicity and well tolerated in human body.[6–8]

Flavonoids, which exist abundantly in edible plants and many folk-medicines, have already received considerable attention as ABC transporter inhibitors.[6] Chalcones, prominent secondary metabolites precursors of flavonoids, displayed similar inhibitory effect on P-gp function as flavonoids.[9,10]

We previously described that a series of bifendate derivatives are more potent than bifendate and verapamil (VRP) in reversing P-gp mediated MDR,[11] and the sixalkoxyl biphenyl moiety in bifendate played a crucial role in its biological activities.[12] Keeping these in mind, and in view of that two aromatic rings joined by a α,β-unsaturated carbonyl system in chalcones also played significant effects in their pharmacological activities, including P-gp inhibitory effect,[13,14] we hypothesized that bifendate scaffold hybridized with chalcone moiety might enhance the P-gp inhibitory effect of bifendate. Therefore, in this paper, we firstly synthesized a series of bifendate–chalcone hybrids (**8a–i**); additionally, considering that introduction of nitrile group to the molecule could enhance MDR reversal effects of P-gp inhibitors,[15] we prepared bifendate–chalcone hybrids (**11a–c**) containing a nitrile substituent in the α, β-unsaturated moiety. Thus, twelve target compounds (Fig. 1) were synthesized, and their ability to reverse P-gp-mediated MDR was subsequently evaluated.

* Corresponding authors. Tel.: +86 10 66932339; fax: +86 10 68159436 (H.P.); tel./fax: +86 25 83271015 (Y.Z.).
E-mail addresses: p_h2002@hotmail.com (H. Peng), zyhtgd@163.com (Y. Zhang).

0968-0896/$ - see front matter © 2012 Elsevier Ltd. All rights reserved.
doi:10.1016/j.bmc.2012.02.050

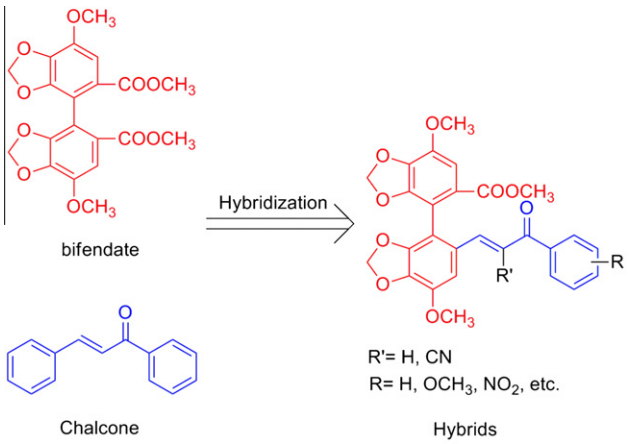

Figure 1. Chemical structures of bifendate, chalcone, and bifendate–chalcone hybrids.

2. Chemistry

The synthetic routes of the target compounds **8a–i** are depicted in Scheme 1. Compounds **1–3** were prepared starting from bifendate by three steps according to literature procedures.[16] Treatment of **3** with imidazole in the presence of 1-(3-dimethylaminopropyl)-3-ethylcarbodiimide hydrochloride (EDCI) and 4-dimeth ylamino-pyridine (DMAP) in CH_2Cl_2 afforded amide **4**, which was then reduced by $NaBH_4$ in THF to give the corresponding hydroxylate **5**. Direct oxidation of **5** with pyridinium chlorochromate (PCC) provided aldehyde **6**. Treatment of **6** with various substituted acetophenones **7a–i** through BF_3-catalyzed Claisen–Schmidt reaction afforded **8a–i**, respectively. The synthetic routes of the target compounds **11a–c** are shown in Scheme 2. Briefly, Claisen-type condensation between the methyl benzoate **9a–c** and acetonitrile gave α-cyano ketones **10a–c**, which was treated with **6** via L-proline-catalyzed Aldol reaction provided **11a–c**, respectively. All the chemical structures of the target compounds are listed in Table 1.

3. Results and discussion

3.1. Biological evaluation

3.1.1. Cytotoxicity assay

Since an ideal P-gp inhibitor should reverse MDR at non-toxic concentrations,[17] the intrinsic cytotoxicity of the target compounds against parental sensitive K562 cells and K562/A02 cells which overexpress P-gp (induced by adriamycin)[18] was determined by MTS assay. Anticancer drug adriamycin (ADR) was served as the

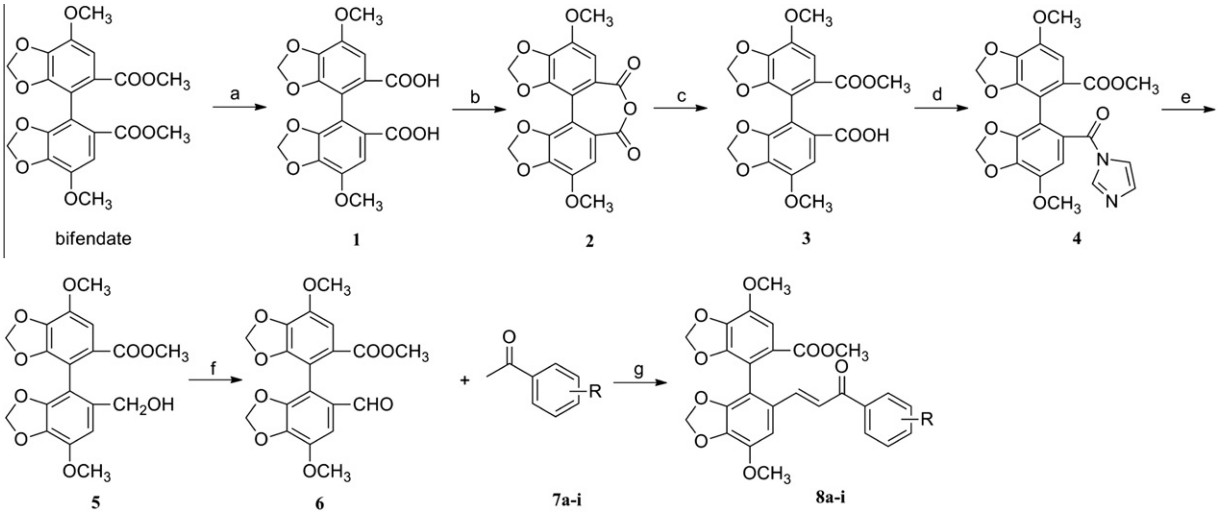

Scheme 1. Synthesis of the target compounds **8a–i**. Reagents and conditions: (a) 10% NaOH, reflux, 5 h; (b) $(Ac)_2O$, reflux, 8 h; (c) CH_3OH, reflux, 3 h; (d) imidazole, EDCI, DMAP, CH_2Cl_2, rt, 2 h; (e) $NaBH_4$, THF/H_2O, 0 °C, 1 h; (f) PCC, CH_2Cl_2, 0 °C, rt, 1 h; (g) BF_3–Et_2O, 1,4-dioxane, 115 °C, 4–5 h.

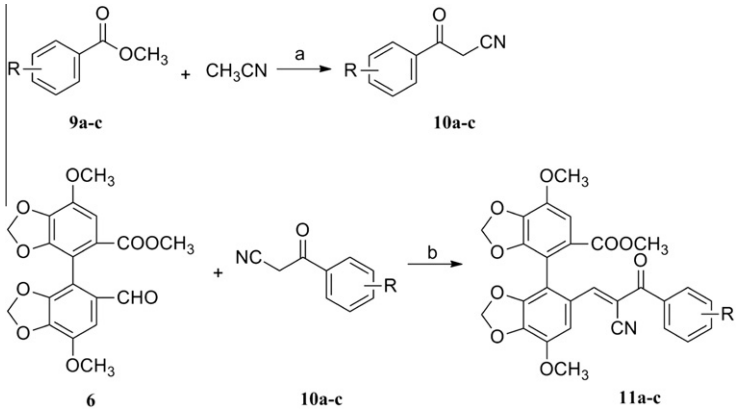

Scheme 2. Synthesis of the target compounds **11a–c**. Reagents and conditions: (a) acetonitrile, 60% NaH, 80 °C, 3 h; (b) L-proline, ethanol, rt, 10 h.

Table 1
Structures of the target compounds

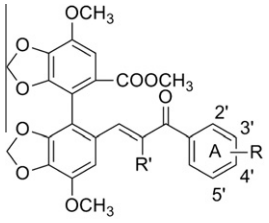

Target compounds

Compound	R′	R substituents: A-ring			
		2′	3′	4′	5′
8a	H	H	H	H	H
8b	H	H	H	OH	H
8c	H	H	H	OCH_3	H
8d	H	OCH_3	H	H	H
8e	H	OCH_3	H	OCH_3	H
8f	H	OCH_3	H	H	OCH_3
8g	H	CH_3	H	H	CH_3
8h	H	H	OCH_3	OCH_3	OCH_3
8i	H	H	H	NO_2	H
11a	CN	H	H	OCH_3	H
11b	CN	H	H	CH_3	H
11c	CN	H	OCH_3	OCH_3	OCH_3

Table 2
IC_{50} values of target compounds against K562 and K562/A02 cells in vitro by MTS assay

Compound	IC_{50}[a] (μM)		Compound	IC_{50}[a] (μM)	
	K562/A02	K562		K562/A02	K562
8a	>100	>100	**8h**	>200	171.8
8b	>100	>100	**8i**	>100	73.37
8c	>100	>100	**11a**	37.21	>100
8d	>200	>200	**11b**	48.36	61.27
8e	>100	>100	**11c**	38.94	60.29
8f	>200	>200	Bifendate	>100	>100
8g	>200	>200	ADR[b]	46.69	0.43

[a] IC_{50} values represent the concentration which results in a 50% decrease in cell growth after 72 h incubation. IC_{50} values are expressed as means of triplicate experiments.
[b] ADR was used as a positive control.

positive control. As shown in Table 2, K562/A02 cells were significantly resistant to ADR (a substrate of P-gp). The IC_{50} value of ADR for K562/A02 cells (46.69 μM) was 108-fold higher than that for K562 cells (0.43 μM). Interestingly, most of the target compounds possessed little (IC_{50} > 100 μM) or slight (IC_{50} = 37.2–73.37 μM) intrinsic cytotoxicity in vitro, indicating that this kind of compounds are suitable candidates for the development of P-gp inhibitors. And in the following MDR reversal experiments, compounds were tested at concentrations below IC_{10}.

3.1.2. Effect of the target compounds on Rh123 accumulation

It is known that P-gp transporter, which overexpresses on the plasma membrane of drug-resistant cells, can rapidly efflux Rhodamine 123 (Rh123, a fluorescent substrate of P-gp) before it enters the cells, resulting in a reduction in the fluorescent signal due to a decrease of Rh123 in the intracellular accumulation. Therefore, we firstly examined the effect of the target compounds (10 μM) on the intracellular accumulation of Rh123 in K562/A02 cells by flow cytometry. The classical P-gp inhibitor verapamil (VRP) was employed as a positive control. As shown in Figure 2A, treatment with VRP (10 μM) significantly increased Rh123 level in K562/A02 cells, showing the value of Rh123 accumulation fold change was 8.1. In comparison, the value of Rh123 accumulation fold change of bifendate was only 1.2, suggesting that bifendate displayed much lower P-gp inhibitory effect than VRP, which is consistent with the previous report.[19] Interestingly, this effect was obviously strengthened by bifendate–chalcone hybrids. As shown in Figure 2A, the Rh123 accumulation fold changes of most target compounds were significantly higher than that of bifendate. Notably, **8d**, **8f** and **8g** dramatically increased the intracellular Rh123 level in K562/A02 cells, and the values of Rh123 accumulation fold change were 8.3, 9.2 and 9.1, respectively, which were even higher than that of VRP.

Next, we further investigated the dose response effects of active compounds **8d**, **8f**, **8g** and **8h** on Rh123 accumulation in K562/A02 and parental sensitive K562 cells by flow cytometry. As expected, VRP, **8d**, **8f**, **8g** and **8h** significantly increased Rh123 accumulation in K562/A02 cells in a dose-dependent manner, while such effect was not observed in P-gp-negative K562 cells (Fig. 2B), suggesting that the effect of these compounds on Rh123 accumulation is likely via inhibiting P-gp function.

3.1.3. Inhibitory effect of 8g on P-gp efflux function

To further support the above presumption, the ability of **8g** to inhibit P-gp efflux function was assayed by detecting intracellular Rh123 according to a previously described method with minor modification.[20] As shown in Figure 3A, the parental sensitive K562 cells retained most of the fluorescence dye Rh123 (Fig. 3 A1), while K562/A02 cells, which overexpress P-gp, could pump the Rh123 out efficiently since little Rh123 was observed in K562/A02 cells after 60-min incubation (Fig. 3 A2). However, the amount of Rh123 in K562/A02 cells treated with **8g** was significantly increased in a dose-dependent manner (Fig. 3 B1–3), and

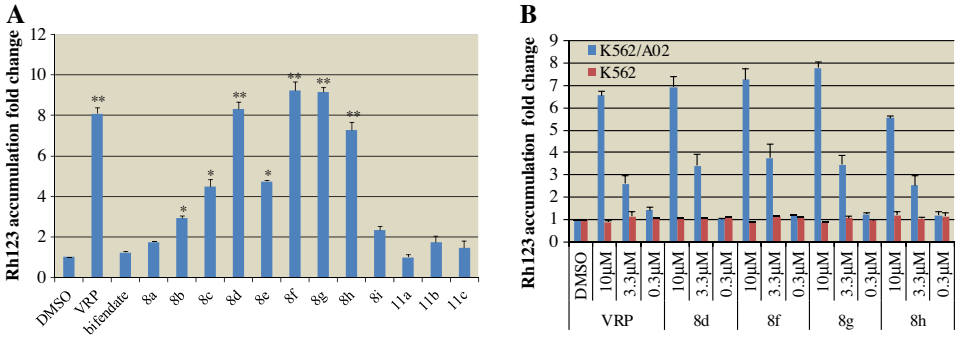

Figure 2. The effect of the target compounds on the intracellular accumulation of Rh123 (0.5 μM). The Rh123 accumulation fold change values were identified by dividing the fluorescence intensity obtained from each measurement by that of control cells (0.1% DMSO) in each cell group, respectively. Data represent means ± S.D. of three independent experiments. $^{*}P$ <0.05, $^{**}P$ <0.01 versus bifendate group.

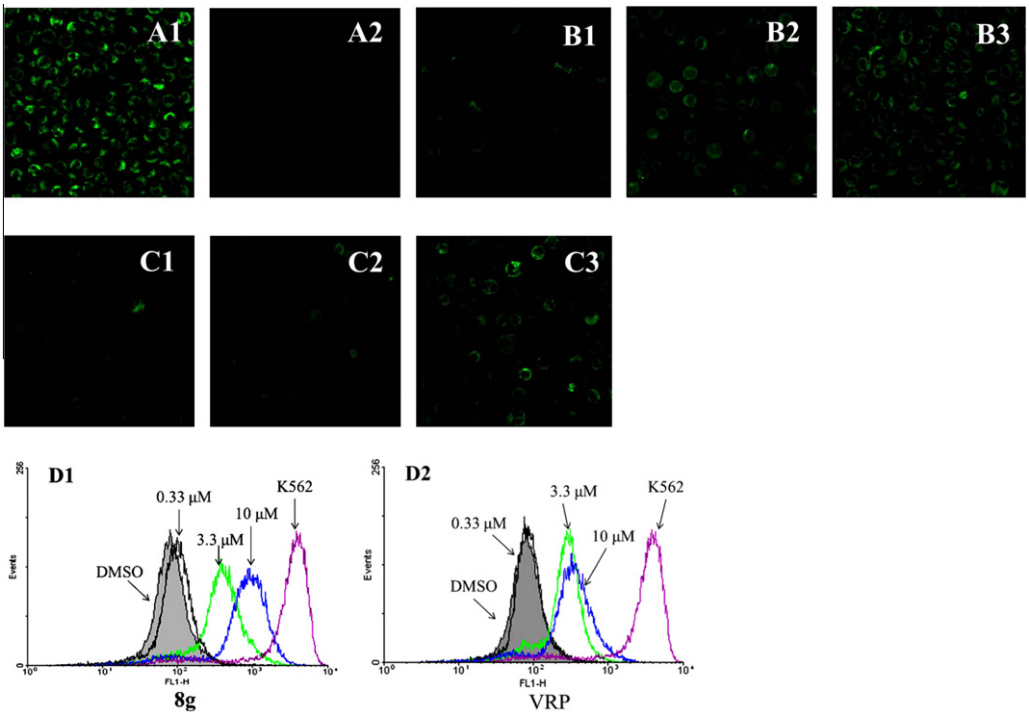

Figure 3. Inhibitory effect of **8g** on P-gp efflux function. K562 cells (A1) or K562/A02 cells (A2, B–C) were incubated with 0.5 μM Rh123 in the presence (B–C) or absence (A) of **8g** (B1: 0.33 μM, B2: 3.3 μM, B3: 10 μM) or VRP (C1: 0.33 μM, C2: 3.3 μM, C3: 10 μM) for 30 min. After treatment, the cells were washed twice with PBS and resuspended in medium, and then incubated at 37 °C for an additional 60 min to allow efflux of the dye. Intracellular Rh123 was then observed and photographed under a fluorescence microscope. (D) Dose–response of **8g** (D1) or VRP (D2, a positive control) in retaining Rh123 accumulation in K562/A02 cells. Intracellular Rh123 was determined by measuring the cell-associated fluorescence using flow cytometry. The purple line represents the level of Rh123 accumulation in K562 cells. 0.1% DMSO was used as vehicle control.

8g displayed much higher potency than VRP at the same doses (Fig. 3 C1–3). Similar results were observed through flow cytometry assay. As shown in Figure 3D, the Rh123 level in K562/A02 cells treated with 0.1% DMSO was much lower than that in K562 cells, however, it was obviously increased by treatment with **8g** in a dose-dependent manner. And treatment with **8g** at 3.3 μM could achieve the similar effect as VRP at 10 μM (Figure 3D). These results verified our assumption that **8g** could effectively inhibit P-gp efflux function, and its potency is much higher than the classical P-gp inhibitor VRP under the same conditions.

3.1.4. Chemo-sensitizing effect of target compounds

Subsequently, we determined chemo-sensitizing effect of the target compounds. Briefly, the cytotoxicity of ADR against K562/A02 and K562 cells was evaluated in the presence or absence of the hybrids at various concentrations (CH: 10 μM, CM: 5 μM and CL: 2.5 μM) by MTS assay, using VRP as the positive control. As shown in Figure 4, both VRP and the target compounds (CH, red bar) at 10 μM displayed little inhibitory effect (<10%) on the survival of K562/A02 and K562 cells. And anticancer drug ADR was non-toxic to K562/A02 and K562 cells at 3.5 μM and 0.2 μM, respectively (Fig. 4, green bar). However, combination treatment with ADR and the target compounds or VRP decreased the survival rate of K562/A02 cells to various extents (Fig. 4A). Notably, **8d**, **8f**, and **8g** exhibited potent chemo-sensitizing effect, and **8g** was the most active. It can be seen from Fig. 4A that 90% or 95% of K562/A02 cells were still surviving by treatment with ADR or **8g** alone, however, the survival rate of the cells was dramatically reduced

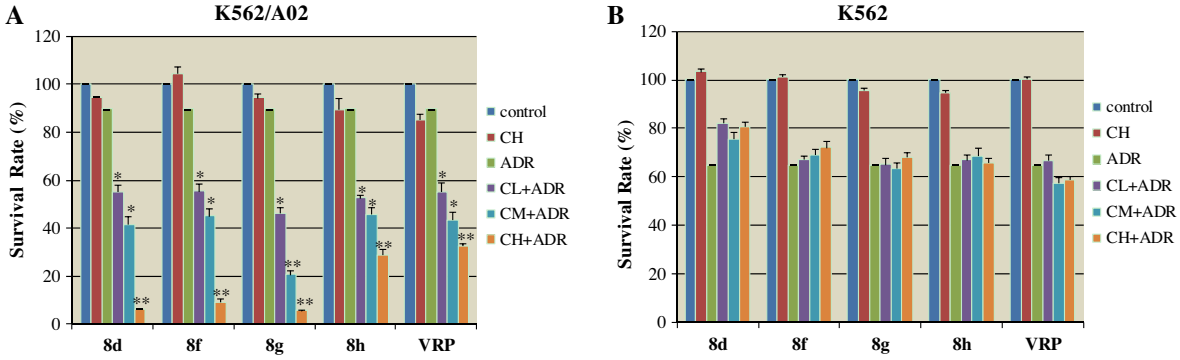

Figure 4. Chemo-sensitizing effect of the active compounds. Drug-resistant K562/A02 (A) and parental K562 (B) cells were treated without or with 3.5 μM and 0.2 μM ADR, respectively, combined with three concentrations (CL: 2.5 μM; CM: 5 μM and CH: 10 μM) of active compound or VRP for 72 h. The survival rates of the cells were determined by MTS assay, and expressed as percentage mean of cell growth ± S.D. with respect to the control without any treatment of three independent experiments. The classical P-gp inhibitor VRP was used as a positive control. $^{*}P$ <0.05, $^{**}P$ <0.01 versus ADR treatment alone group.

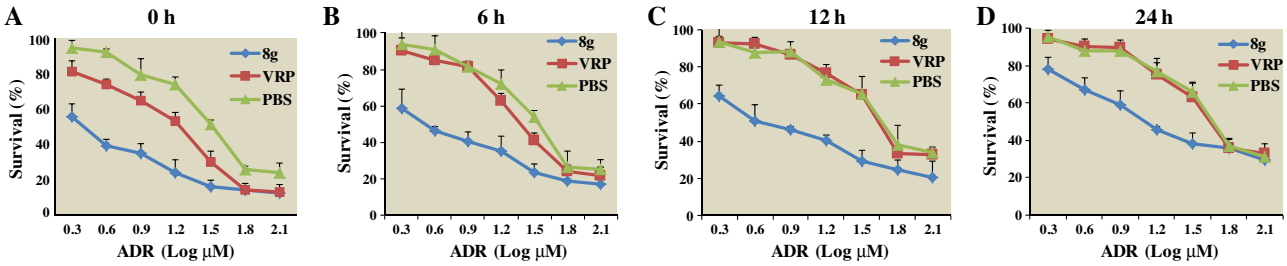

Figure 5. Duration of chemo-sensitizing effect of **8g** and VRP toward ADR in K562/A02 cells after incubation and subsequent washout. K562/A02 cells were incubated with 10 μM **8g** or VRP for 24 h, and then each compound in the culture media was washed out, and the cells were transferred to compound-free fresh media. Various concentrations of ADR was then added to the culture at different time points 0 h (A), 6 h (B), 12 h (C), or 24 h (D) after the removal of the compounds, and incubated for additional 72 h. Cell proliferation was determined by MTS assay. Data represents means ± S.E. of triplicate determinations.

to 46%, 20% and 5% by combination treatment with ADR (3.5 μM) and **8g** at 2.5, 5 and 10 μM, respectively. On the other hand, VRP displayed much weaker chemo-sensitizing effect compared with **8g** under the same conditions. Even if K562/A02 cells were treated with VRP at 10 μM, the survival rate was still higher than 32%. Obviously, **8g** was more potent than the classical P-gp inhibitor VRP, and such chemo-sensitizing effect was not observed in P-gp-negative K562 cells (Fig. 4B), suggesting that bifendate–chalcone hybrids may exert chemo-sensitizing effect by inhibition of P-gp.

3.1.5. Duration of chemo-sensitizing effect of 8g toward ADR in K562/A02 cells

Next, we selected the most active compound **8g** to determine the duration of such chemo-sensitizing effect according to the procedure previously described.[20] Firstly, K562/A02 cells were incubated with 10 μM **8g** or VRP for 24 h, and then each compound in the culture media was washed out, and the cells were transferred to compound-free fresh media. Various concentrations of ADR was then added to the culture at different time points (0, 6, 12, or 24 h) after the removal of the compounds, and incubated for additional 72 h. Cell proliferation was determined by MTS assay to examine the duration of the MDR-reversal activity of **8g** or VRP. As shown in Figure 5, the IC_{50}s of ADR towards K562/A02 cells which were in the absence of treatment with **8g** or VRP, were 33.59, 35.15, 54.11, and 51.67 μM at the following time points 0, 6, 12, or 24 h, respectively. Both **8g** and VRP significantly sensitized K562/A02 cells to ADR right after they were removed, the IC_{50}s of ADR were 2.15 and 12.92 μM, respectively (Fig. 5. A). The IC_{50}s of ADR were 26.06, 51.05 and 51.40 μM, respectively, when addition was at the time points 6, 12 and 24 h after the removal of VRP. These IC_{50}s were almost equal to those obtained in the control group (PBS) which was not exposed to any compounds, suggesting that the chemo-sensitizing effect of VRP may last no more than 6 h. In sharp contrast, **8g** exhibited significant reversal activity even at 24 h after exposure. When ADR was added to the cells at the time points 6, 12, and 24 h after **8g** was removed, its IC_{50}s were 3.57, 5.80, and 17.04 μM, respectively. These data indicated that **8g** displayed potent chemo-sensitizing effect and persisted for much longer time (>24 h) compared with positive control VRP (<6 h) after they were removed from the culture.

3.1.6. Effect of target compounds on the expression of P-gp at mRNA and protein levels

It is believed that inhibiting transport function of P-gp and/or decreasing its expression level could reverse P-gp-mediated MDR.[21] We next examined whether these active compounds, hybrids **8d**, **8f** and **8g**, could decrease the expression of P-gp at mRNA and protein levels by RT-PCR and Western blot analyses, respectively. It can be seen from Figure 6 that there was no marked changes in P-gp expression at mRNA (Fig. 6A) or protein level (Fig. 6B) in K562/A02 cells treated with target compounds (10 μM) for 72 h compared with the vehicle control (0.1% DMSO). These results suggest that the bifendate–chalcone hybrids may reverse P-gp-mediated MDR by inhibiting P-gp efflux function and not by decreasing P-gp expression.

3.1.7. Effect of 8g on P-gp ATPase activity

P-gp normally requires energy from ATP hydrolysis by the ATPase, and this enzyme is typically activated for transportation by P-gp substrates. Some identified reversal agents (e.g., VRP) also stimulated the basal ATPase activity, thus behaving like a substrate or competitive inhibitor for the pumps,[22] namely, it competes with the cytotoxic drugs for efflux by the P-gp. Therefore, a high concentration of such drug is necessary to maintain the MDR-reversal effect. In this case, it might easily reach toxic ranges, leading to a serious side effect.[23] Therefore, the effect of **8g** on P-gp ATPase activity was determined to examine whether it is a P-gp substrate according to a previously described method.[24] Briefly, the activity of P-gp ATPase was measured in the presence or absence of Na_3VO_4 (as an inhibitor control), **8g**, or VRP (as a substrate control). Then, the luminescence of each sample was detected in a luminometer.

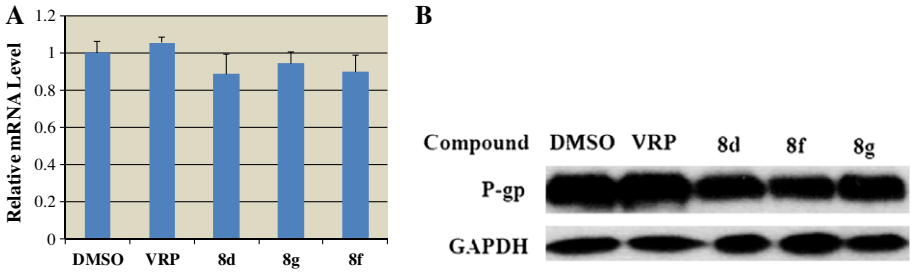

Figure 6. (A) Effects of active compounds on P-gp mRNA level. The relative P-gp mRNA level treated with compounds was expressed as fold change of the control cultures (in the presence of 0.1% DMSO). Data shown are mean ± S.D. from three independent experiments. (B) Effects of active compounds on P-gp protein expression level. Independent experiments were performed at least three times by Western blot, and a representative experiment is shown.

Table 3
Effect of **8g** on P-gp ATPase activity

Drug	Concentration (μM)	Luminescence[a] (relative light units)
Untreated	0	242,328 ± 1398
VRP	200	231,282 ± 293*
Na_3VO_4	200	281,688 ± 439*
8g	40	271,290 ± 2480*

[a] Relative light units represent the level of ATP in the sample, exhibiting a negative relationship with activity of P-gp ATPase. Data are expressed as means ± S.D.s of three separate experiments.
* p <0.01 versus untreated group, determined by Student's t test.

And, the luminescence value of each sample represents its ATP level, which is negatively correlated with the activity of P-gp ATPase. As shown in Table 3, VRP caused a significant increase in the activity of P-gp ATPase (P <0.01) compared with the untreated group, while **8g** or Na_3VO_4 showed no stimulation of the P-gp ATPase activity, indicating that **8g** was not a P-gp substrate.

3.2. Structure–activity relationships

As mentioned above, the bifendate–chalcone hybrids exhibited potent P-gp inhibitory effect, and several compounds possessed activity comparable to or even stronger than classical P-gp inhibitor VRP. It was obvious that R substitutes at benzene ring (A-ring) of chalcone moiety (Table 1) played an important role in the P-gp-mediated MDR reversal activity. Firstly, the compounds with a methoxy group in the A-ring usually showed more potent inhibitory effect than those bearing a hydroxy or nitro group (**8c** vs **8b** and **8i**). Secondly, compounds with a methoxy group at the ortho or meta position of the A-ring exhibited better activity than those with a *para*-methoxy group (**8d** vs **8c**, **8f** vs **8e**). Thirdly, changing the methoxy group into methyl group could further improved the P-gp inhibitory activity (**8g** vs **8e**, **11b** vs **11a**), and the compound **8g** was the most active. Fourthly, when a nitrile group was introduced into the α,β-unsaturated moiety of the hybrids, the P-gp inhibitory activity was significantly reduced (**8c** vs **11a**, **8h** vs **11c**), probably because the introduction of nitrile group might change the electron density distribution of the hybrids, thus decreasing the affinity with P-gp. However, the precise SARs could be drawn only when further investigation will be completed.

4. Conclusions

In summary, a series of novel bifendate–chalcone hybrids were synthesized and their inhibitory effect on P-gp was evaluated using the classical P-gp inhibitor VRP as a positive control. Most of the target compounds exhibited strong P-gp inhibitory effect than the lead compound bifendate, and compounds **8d, 8f** and **8g** more potently reversed P-gp-mediated MDR than VRP through blocking the drug efflux function of P-gp. Further study showed that **8g** did not inhibit expression of P-gp at mRNA and protein levels. Additionally, the chemo-sensitizing effect of **8g** persisted much longer (>24 h) than that of VRP (<6 h). And, unlike VRP, **8g** showed no stimulation of the P-gp ATPase activity, suggesting it was not a P-gp substrate. Besides, the intrinsic cytotoxicity of **8g** was very low (IC_{50} > 200 μM) in vitro, therefore, **8g** might represent a promising lead to develop P-gp-mediated MDR reversal agents in cancer chemotherapy.

5. Experimental protocols

5.1. Chemical analysis

Melting points were determined on a Mel-TEMP II melting point apparatus which was uncorrected. All of the synthesized compounds were purified by column chromatography (CC) on silica gel (200–300 mesh). Analytical TLC was performed on GF/UV 254 plates and the chromatograms were visualized under UV light at 254 and 365 nm. Subsequently, all the compounds were routinely analyzed by IR (Shimadzu FTIR-8400S), ^{1}H NMR and ^{13}C NMR (Bruker ACF-300Q, 300 MHz), and MS (Hewlett–Packard 1100 LC/MSD spectrometer). High resolution mass spectra (HRMS) were recorded on Agilent technologies LC/MSD TOF. All solvents were reagent grade and, when necessary, were purified and dried by standards methods. Compounds **1–3** were synthesized as previously described.[16] Compounds **7a–i** and **9a–c** were commercially available.

5.2. Synthesis of methyl 5′-(1*H*-imidazole-1-carbonyl)-7,7′-dimethoxy-{4,4′-bibenzo[*d*][1,3]dioxole}-5-carboxylate 4

To a solution of compound **3** (2 g, 5.0 mmol) in dry CH_2Cl_2 (50 mL), imidazole (404 mg, 5.9 mmol), EDCI (1.1 g, 5.9 mmol) and DMAP (61 mg, 0.5 mmol) was added, and the mixture was stirred at room temperature for 2 h. The reaction solution was diluted with water and extracted with CH_2Cl_2. The organic layer was washed sequentially with 1 N HCl, saturated $NaHCO_3$ solution and brine, then dried with sodium sulfate, filtered and evaporated in vacuo to give corresponding crude compound **4** (98%), which was used in the next without other purification.

5.3. Synthesis of methyl 5′-(hydroxymethyl)-7,7′-dimethoxy-{4,4′-bibenzo[*d*][1,3]dioxole}-5-carboxylate 5

A water solution of $NaBH_4$ (332 mg, 8.8 mmol) was dropped to the stirred solution of compound **4** (2 g, 4.4 mmol) in THF 30 mL at 0 °C. The reaction mixture was stirred for 1 h at room temperature. After the completion of reaction, 10% aqueous HCl was added slowly to the mixture until no hydrogen generated. The mixture was filtered and washed with CH_2Cl_2 several times. The filtrate was diluted with water and extracted with CH_2Cl_2. The organic layer was washed with brine, dried with anhydrous sodium sulfate, filtered and evaporated in vacuum. The crude product was purified by chromatography (PE/EtOAc = 5:3) to afford the title compound **5** (1.6 g). As a white solid, yield: 92%; mp: 126–128 °C. Analytical data for **5**: ^{1}H NMR ($CDCl_3$, 300 MHz, δ ppm): 3.71 (s, 3H, $COOCH_3$), 3.95 (s, 3H, Ar-OCH_3), 3.97 (s, 3H, $ArOCH_3$), 4.35 (d, 1H, C**H**$_2$OH, J = 12 Hz), 4.40 (d, 1H, C**H**$_2$OH, J = 12 Hz), 5.91–6.04 (m, 4H, 2 × OCH_2O), 6.78 (s, 1H, Ar-H), 7.33 (s, 1H, Ar-H). ESI-MS m/z: 413 $[M+Na]^+$.

5.4. Synthesis of methyl 5′-formyl-7,7′-dimethoxy-{4,4′-bibenzo[*d*][1,3]dioxole}-5-carboxylate 6

Compound **5** (1.5 g, 3.8 mmol) was dissolved in CH_2Cl_2 (30 mL), and cooled to 0 °C. PCC (900 mg, 4.2 mmol) was added and the solution was stirred for 1 h at rt. Then, the mixture was filtered through Celite, and washed with CH_2Cl_2. The solvent was removed under reduced pressure and the crude product was purified by flash chromatography (PE/EtOAc = 3:1) gave the title compound **6** (1.46 g). As a white solid, yield: 98%; mp: 179–181 °C. Analytical data for **6**: ^{1}H NMR ($CDCl_3$, 300 MHz, δ ppm): 3.68 (s, 3H, $COOCH_3$), 3.98 (s, 3H, $ArOCH_3$), 3.99 (s, 3H, $ArOCH_3$), 6.01–6.10 (m, 4H, 2 × OCH_2O), 7.32 (s, 1H, Ar-H), 7.42 (s, 1H, Ar-H); ^{13}C NMR ($CDCl_3$, 75 MHz, δ ppm): δ 52.1 (COO**C**H$_3$), 56.5 (OCH_3), 56.8 (OCH_3), 102.6 (OCH_2O), 102.7 (OCH_2O), 107.7, 108.2, 111.9, 114.1, 124.5, 128.7, 138.3, 139.9, 143.2, 143.7, 147.0, 148.1, 166.1 (**C**$OOCH_3$), 189.5 (CHO); IR (KBr, cm^{-1}): ν 3007, 2903, 2358, 1710, 1682, 1632, 1579, 1484, 1455, 1416, 1406, 1352, 1306, 1255, 1156, 1100, 1039, 928, 858, 757; ESI-MS m/z: 411 $[M+Na]^+$; HRMS (ESI m/z) for $C_{19}H_{16}O_9Na$ calcd 411.0692, found 411.0696 $[M+Na]^+$.

5.5. General procedure for the preparation of 8a–i

BF_3–Et_2O was added (35.6 μL, 0.13 mmol) to the stirred solution of compound **6** (100 mg, 0.26 mmol) and various substituted acetophenones **7a**–**i** (0.28 mmol) in dry 1,4-dioxane at room temperature under a nitrogen atmosphere. The reaction mixture was stirred and refluxed for 4–5 h at 115 °C and cooled to room temperature. And then, the reaction mixture was diluted with saturated aqueous $NaHCO_3$ and extracted with EtOAc. The organic layer was washed with brine, dried with anhydrous sodium sulfate, filtered and evaporated in vacuum. The crude product was purified by column chromatography (PE/EtOAc = 10:1–1:1) to yield the title compounds, respectively.

5.5.1. (*E*)-Methyl 7,7′-dimethoxy-5′-(3-oxo-3-phenylprop-1-en-1-yl)-{4,4′-bibenzo[*d*][1,3] dioxole}-5-carboxylate (8a)

The title compound was obtained starting from **6** and acetophenone. As a yellow solid, yield: 70%; mp: 141–143 °C. Analytical data for **8a**: ^{1}H NMR ($CDCl_3$, 300 MHz, δ ppm): 3.67 (s, 3H, $COOCH_3$), 3.99 (s, 3H, $ArOCH_3$), 4.00 (s, 3H, $ArOCH_3$), 5.96–6.08 (m, 4H, 2 × OCH_2O), 7.08 (s, 1H, Ar-H), 7.25 (d, 1H, CH=C*H*CO, J = 15.0 Hz), 7.41 (s, 1H, Ar-H), 7.44–7.48 (m, 2H, Ar-H), 7.54 (d, 1H, C*H*=CHCO, J = 15.1 Hz), 7.52–7.58 (m, 1H, Ar-H), 7.88 (d, 2H, Ar-H, J = 7.8 Hz); ^{13}C NMR ($CDCl_3$, 75 MHz, δ ppm): δ 52.1 (COO**C**H_3), 56.6 (OCH_3), 56.7 (OCH_3), 102.2 (OCH_2O), 102.5 (OCH_2O), 106.3, 110.0, 111.8, 112.3, 121.7 (CH=*C*HCO), 124.3, 128.1, 128.4 (2 × ArC), 128.5 (2 × ArC), 132.6, 136.9, 138.2, 138.5, 142.9 (*C*H=CHCO), 143.0, 143.4, 147.1, 147.8, 166.1 (*C*$OOCH_3$), 190.5 (CH=CH*C*O); IR (KBr, cm^{-1}): ν 2945, 2368, 1718, 1654, 1636, 1584, 1447, 1432, 1416, 1353, 1173, 1100, 1042, 933, 757; ESI-MS: m/z 491.1 $[M+H]^+$; HRMS (ESI m/z) for $C_{27}H_{23}O_9$ calcd 491.1342, found 491.1344 $[M+H]^+$.

5.5.2. (*E*)-Methyl 5′-(3-(4-hydroxyphenyl)-3-oxoprop-1-en-1-yl)-7,7′-dimethoxy-{4,4′-bibenzo [*d*][1,3]dioxole}-5-carboxylate (8b)

The title compound was obtained starting from **6** and 4′-hydroxyacetophenone. As a yellow solid, yield: 72%; mp: 248–250 °C. Analytical data for **8b**: ^{1}H NMR (DMSO, 300 MHz, δ ppm): 3.57 (s, 3H, $COOCH_3$), 3.95 (s, 3H, $ArOCH_3$), 3.99 (s, 3H, $ArOCH_3$), 5.89–6.07 (m, 4H, 2 × OCH_2O), 6.86 (s, 1H, Ar-H), 6.89 (s, 1H, Ar-H), 7.28–7.45 (m, 3H, 2×Ar-H, CH=C*H*CO), 7.70 (d, 1H, C*H*=CHCO, J = 15.6 Hz), 7.97 (d, 2H, Ar-H, J = 7.8 Hz), 10.39 (s, 1H, OH); ^{13}C NMR (DMSO, 75 MHz, δ ppm): δ 51.9 (COO*C*H_3), 56.4 (OCH_3), 56.5 (OCH_3), 101.9 (OCH_2O), 102.4 (OCH_2O), 106.2, 109.4, 110.9, 111.9, 115.2 (2 × ArC), 121.1 (CH=*C*HCO), 124.4, 127.6, 129.1, 131.0 (2 × ArC), 136.2, 137.8, 140.2 (*C*H=CHCO), 142.5, 143.0, 146.5, 147.5, 162.1, 165.5 (*C*$OOCH_3$), 186.9 (CH=CH*C*O); IR (KBr, cm^{-1}): ν 3244, 2359, 1708, 1635, 1605, 1586, 1558,1635, 1442,1431, 1236, 1209, 1165, 1134, 1040, 927, 841; ESI-MS: m/z 507.0 $[M+H]^+$; HRMS (ESI m/z) for $C_{27}H_{23}O_{10}$ calcd 507.1291, found 507.1293 $[M+H]^+$.

5.5.3. (*E*)-Methyl 7,7′-dimethoxy-5′-(3-(4-methoxyphenyl)-3-oxoprop-1-en-1-yl)-{4,4′-bibenzo[*d*][1,3]dioxole}-5-carboxylate (8c)

The title compound was obtained starting from **6** and 4′-methoxyacetophenone. As a yellow solid, yield: 81%; mp: 172–174 °C. Analytical data for **8c**: ^{1}H NMR ($CDCl_3$, 300 MHz, δ ppm): 3.67 (s, 3H, OCH_3), 3.87 (s, 3H, OCH_3), 3.99 (s, 3H, OCH_3), 4.01 (s, 3H, OCH_3), 5.95–6.02 (m, 4H, 2 × OCH_2O), 6.92 (d, 2H, 2 × Ar-H, J = 8.7 Hz), 7.07 (s, 1H, Ar-H), 7.27 (d, 1H, CH=C*H*CO, J = 15.6 Hz), 7.41 (s, 1H, Ar-H), 7.53 (d, 1H, C*H*=CHCO, J = 15.6 Hz), 7.91 (d, 2H, 2 × Ar-H, J = 8.7 Hz); ^{13}C NMR ($CDCl_3$, 75 MHz, δ ppm): δ 52.1 (COO*C*H_3), 55.5 (OCH_3), 56.7 (OCH_3), 56.8 (OCH_3), 102.2 (OCH_2O), 102.6 (OCH_2O), 106.3, 110.1, 111.9, 112.2, 113.8 (2 × ArC), 121.6 (CH=*C*HCO), 124.4, 128.4, 130.7 (2 × ArC), 131.2, 136.8, 138.6, 142.0 (*C*H=CHCO), 143.1, 143.4, 147.2, 147.8, 163.1, 166.1 (*C*$OOCH_3$), 188.7 (CH=CH*C*O); IR (KBr, cm^{-1}): ν 2946, 1713, 1655, 1635, 1603, 1582, 1432, 1417, 1352, 1320, 1250, 1171, 1101, 1042, 926, 828, 759; ESI-MS: m/z 521 $[M+H]^+$, 543 $[M+Na]^+$; HRMS (ESI m/z) for $C_{28}H_{25}O_{10}$ calcd 521.1448, found 521.1450 $[M+H]^+$.

5.5.4. (*E*)-Methyl 7,7′-dimethoxy-5′-(3-(2-methoxyphenyl)-3-oxoprop-1-en-1-yl)-{4,4′-bibenzo[*d*][1,3]dioxole}-5-carboxylate (8d)

The title compound was obtained starting from **6** and 2′-methoxyacetophenone. As a yellow solid, yield: 63%; mp: 74–76 °C. Analytical data for **8d**: ^{1}H NMR ($CDCl_3$, 300 MHz, δ ppm): 3.66 (s, 3H, OCH_3), 3.93 (s, 3H, OCH_3), 3.97 (s, 3H, OCH_3), 3.98 (s, 3H, OCH_3), 5.92–6.00 (m, 4H, 2 × OCH_2O), 6.90–6.98 (m, 2H, 2 × Ar-H), 7.03 (s, 1H, Ar-H), 7.10 (d, 1H, CH=C*H*CO, J = 15.7 Hz), 7.30–7.46 (m, 4H, C*H*=CHCO, 3 × Ar-H); ^{13}C NMR ($CDCl_3$, 75 MHz, δ ppm): δ 52.0 (COO**C**H_3), 55.6 (OCH_3), 56.5 (OCH_3), 56.7 (OCH_3), 102.1 (OCH_2O), 102.4 (OCH_2O), 106.0, 110.0, 111.5, 111.8, 111.2, 120.5 (CH=*C*HCO), 124.3, 126.5, 128.2, 129.3, 130.0, 132.4, 136.7, 138.4, 141.9 (*C*H=CHCO), 142.9, 143.3, 147.0, 147.7, 157.8, 166.1 (*C*$OOCH_3$), 193.0 (CH=CH**C**O); IR (KBr, cm^{-1}): ν 2938, 1720, 1635, 1598, 1582, 1484, 1416, 1352, 1322, 1290, 1245, 1173, 1100, 1042, 926, 757; ESI-MS: m/z 521 $[M+H]^+$, 543 $[M+Na]^+$; HRMS (ESI m/z) for $C_{28}H_{25}O_{10}$ calcd 521.1448, found 521.1449 $[M+H]^+$.

5.5.5. (*E*)-Methyl 5′-(3-(2,4-dimethoxyphenyl)-3-oxoprop-1-en-1-yl)-7,7′-dimethoxy-{4,4′-bibenzo[*d*][1,3]dioxole}-5-carboxylate (8e)

The title compound was obtained starting from **6** and 2′,4′-dimethoxyacetophenone. As a yellow solid, yield: 41%; mp: 86–88 °C. Analytical data for **8e**: ^{1}H NMR ($CDCl_3$, 300 MHz, δ ppm): 3.66 (s, 3H, OCH_3), 3.83 (s, 6H, 2 × OCH_3), 3.85 (s, 3H, OCH_3), 3.98 (s, 6H, 2 × OCH_3), 5.96–6.01 (m, 4H, 2 × OCH_2O), 6.44 (d, 1H, Ar-H, J = 2.0 Hz), 6.49–6.52 (m, 1H, Ar-H), 7.11 (s, 1H, Ar-H), 7.25 (d, 1H, CH=C*H*CO, J = 15.6 Hz), 7.38 (s, 1H, Ar-H), 7.41 (d, 1H, C*H*=CHCO, J = 15.6 Hz). 7.61 (d, 1H, Ar-H, J = 8.6 Hz); ^{13}C NMR ($CDCl_3$, 75 MHz, δ ppm): δ 52.0 ($COOCH_3$), 55.5 (OCH_3), 55.6 (OCH_3), 56.5 (OCH_3), 56.7 (OCH_3), 98.7, 102.0 (OCH_2O), 102.4 (OCH_2O), 105.0, 106.1, 110.2, 111.8, 112.1, 122.3, 124.4, 126.7 (CH=*C*HCO), 128.7, 132.6, 136.5, 138.5, 140.4 (*C*H=CHCO), 142.9, 143.3, 147.1, 147.8, 160.2, 164.8, 166.1 (*C*$OOCH_3$), 190.4 (CH=CH**C**O); IR (KBr, cm^{-1}): ν 2359, 1718, 1636, 1608, 1412, 1383, 1355, 1326, 1253, 1163, 1097, 1040, 926, 665; ESI-MS: m/z 551 $[M+H]^+$, 573 $[M+Na]^+$; HRMS (ESI m/z) for $C_{29}H_{27}O_{11}$ calcd 551.1553, found 551.1556 $[M+H]^+$.

5.5.6. (*E*)-Methyl 5′-(3-(2,5-dimethoxyphenyl)-3-oxoprop-1-en-1-yl)-7,7′-dimethoxy-{4,4′-bibenzo[*d*][1,3]dioxole}-5-carboxylate (8f)

The title compound was obtained starting from **6** and 2′,5′-dimethoxyacetophenone. As a yellow solid, yield: 58%; mp: 65–67 °C. Analytical data for **8f**: ^{1}H NMR ($CDCl_3$, 300 MHz, δ ppm): 3.66 (s, 3H, $COOCH_3$), 3.77 (s, 6H, 2 × $ArOCH_3$), 3.97 (s, 6H, 2 × $ArOCH_3$), 5.90–6.04 (m, 4H, 2 × OCH_2O), 6.78–6.84 (m, 1H, Ar-H), 6.94–6.98 (m, 1H, Ar-H), 7.03 (s, 2H, Ar-H), 7.15 (d, 1H, CH=C*H*CO, J = 15.0 Hz), 7.44–7.48 (m, 2H, Ar-H), 7.34 (d, 1H, C*H* =CHCO, J = 15.1 Hz), 7.37 (s, 1H, Ar-H); ^{13}C NMR ($CDCl_3$, 75 MHz, δ ppm): δ 52.0 (COO**C**H_3), 55.8 (OCH_3), 56.4 (OCH_3), 56.5 (OCH_3), 56.7 (OCH_3), 102.1 (OCH_2O), 102.5 (OCH_2O), 106.0, 109.9, 111.7, 113.2, 114.4, 118.4 (CH=CHCO), 124.3, 126.3, 128.2, 129.8, 136.7, 138.4, 141.9 (*C*H=CHCO), 142.9, 143.3, 147.1, 147.7, 152.2, 153.5, 166.1 (*C*$OOCH_3$), 192.5 (CH=CHCO); IR (KBr, cm^{-1}): ν 2359, 1636, 1413, 1384, 1171, 1102, 1048, 763; ESI-MS: m/z 551.0 $[M+H]^+$; HRMS (ESI m/z) for $C_{29}H_{27}O_{11}$ calcd 551.1553, found 551.1556 $[M+H]^+$.

5.5.7. (*E*)-Methyl 5′-(3-(2,4-dimethylphenyl)-3-oxoprop-1-en-1-yl)-7,7′-dimethoxy-{4,4′-bibenzo[*d*][1,3]dioxole}-5-carboxylate (8g)

The title compound was obtained starting from **6** and 2′, 4′-dimethylacetophenone. As a yellow solid, yield: 68%; mp: 76–78 °C. Analytical data for **8g**: ^{1}H NMR ($CDCl_3$, 300 MHz, δ ppm): 2.33 (s, 6H, 2 × CH_3), 3.67 (s, 3H, OCH_3), 3.97 (s, 3H, OCH_3), 3.98 (s, 3H, OCH_3), 4.01 (s, 3H, OCH_3), 5.93–6.01 (m, 4H, 2 × OCH_2O), 6.91 (d, 1H, CH=C*H*CO, J = 15.9 Hz), 6.92–7.02 (m, 3H, 3 × Ar-H), 7.22 (d, 1H, C*H*=CHCO, J = 15.9 Hz), 7.24–7.28 (m, 1H, Ar-H), 7.37 (s, 1H, Ar-H); ^{13}C NMR ($CDCl_3$, 75 MHz, δ ppm): δ 20.3 (CH_3), 21.3 (CH_3), 52.0 (COO*C*H_3), 56.5 (OCH_3), 56.7 (OCH_3), 102.2 (OCH_2O), 102.5 (OCH_2O), 105.9, 109.9, 111.8, 112.2, 124.3, 125.8 (CH=*C*HCO), 126.1, 127.9, 128.4, 132.0, 136.1, 136.9, 137.2, 138.4, 140.6, 143.0, 143.4, 143.6 (*C*H=CHCO), 147.1, 147.6, 166.0 (*C*OOCH$_3$), 195.9 (CH=CH*C*O); IR (KBr, cm^{-1}): ν 2918, 1719, 1636, 1583, 1432, 1416, 1354, 1173, 1101, 1042, 936, 821, 762; ESI-MS: m/z 519 [M+H]$^+$, 541 [M+Na]$^+$; HRMS (ESI m/z) for $C_{29}H_{27}O_9$ calcd 519.1655, found 519.1656 [M+H]$^+$.

5.5.8. (*E*)-Methyl 7,7′-dimethoxy-5′-(3-oxo-3-(3,4,5-trimethoxyphenyl)prop-1-en-1-yl)-{4,4′-bibenzo[*d*][1,3]dioxole}-5-carboxylate (8h)

The title compound was obtained starting from **6** and 3′,4′, 5′-trimethoxyacetophenone. As a yellow solid, yield: 61%; mp: 80–82 °C. Analytical data for **8h**: ^{1}H NMR ($CDCl_3$, 300 MHz, δ ppm): 3.68 (s, 3H, OCH_3), 3.90 (s, 6H, 2 × OCH_3), 3.91 (s, 3H, OCH_3), 3.98 (s, 3H, OCH_3), 4.01 (s, 3H, OCH_3), 5.98–6.02 (m, 4H, 2 × OCH_2O), 7.05 (s, 1H, Ar-H), 7.15 (s, 2H, 2 × Ar-H), 7.19 (d, 1H, CH=C*H*CO, J = 15.5 Hz), 7.41 (s, 1H, Ar-H), 7.61 (d, 1H, C*H*=CHCO, J = 15.5 Hz); ^{13}C NMR ($CDCl_3$, 75 MHz, δ ppm): δ 52.0 (COO*C*H_3), 56.4 (2 × OCH_3), 56.7 (OCH_3), 56.8 (OCH_3), 60.9 (OCH_3), 102.1 (OCH_2O), 102.5 (OCH_2O), 106.2 (2 × ArC), 107.7, 110.2, 111.9, 112.0, 121.2 (CH=*C*HCO), 124.3, 128.2, 133.6, 136.9, 138.5, 142.9 (*C*H=CHCO), 143.0, 143.3, 146.3, 147.3, 147.7, 153.1 (2 × ArC), 166.0 (*C*OOCH$_3$), 188.8 (CH=CH*C*O); IR (KBr, cm^{-1}): ν 3004, 2930, 1719, 1635, 1577, 1432, 1414, 1348, 1321, 1192, 1173, 1158, 1127, 1100, 1043, 926, 836, 751; ESI-MS: m/z 581 [M+H]$^+$, 603 [M+Na]$^+$; HRMS (ESI m/z) for $C_{30}H_{29}O_{12}$ calcd 581.1659, found 581.1663 [M+H]$^+$.

5.5.9. (*E*)-Methyl 7,7′-dimethoxy-5′-(3-(4-nitrophenyl)-3-oxoprop-1-en-1-yl)-{4,4′-bibenzo[*d*] [1,3]dioxole}-5-carboxylate (8i)

The title compound was obtained starting from **6** and 4′-nitroacetophenone. As a yellow solid, yield: 45%; mp: 183–185 °C. Analytical data for **8i**: ^{1}H NMR ($CDCl_3$, 300 MHz, δ ppm): 3.69 (s, 3H, OCH_3), 4.00 (s, 3H, OCH_3), 4.01 (s, 3H, OCH_3), 6.01 (s, 4H, 2 × OCH_2O), 7.08 (s, 1H, Ar-H), 7.17 (d, 1H, CH=C*H*CO, J = 15.7 Hz), 7.42 (s, 1H, Ar-H), 7.54 (d, 1H, C*H*=CHCO, J = 15.6 Hz), 7.98 (d, 2H, 2 × Ar-H, J = 8.1 Hz), 8.28 (d, 2H, 2 × Ar-H, J = 8.7 Hz); ^{13}C NMR ($CDCl_3$, 75 MHz, δ ppm): δ 52.1 (COO*C*H_3), 56.7 (2 × OCH_3), 102.3 (OCH_2O), 102.5 (OCH_2O), 106.6, 109.7, 111.8, 111.8, 112.7, 120.9 (CH=*C*HCO), 123.7 (2 × ArC), 124.3, 127.5, 129.3 (2 × ArC), 137.6, 138.5, 143.1, 1432, 143.4, 144.9 (*C* H=CHCO),147.8, 149.9, 150.6, 166.0 (*C*OOCH$_3$), 193.0 (CH=CH**C**O); IR (KBr, cm^{-1}): ν 2359, 1706, 1636, 1575, 1384, 1322, 1175, 1097, 1048, 926, 840, 706; ESI-MS: m/z 536 [M+H]$^+$, 558 [M+Na]$^+$; HRMS (ESI m/z) for $C_{27}H_{22}NO_{11}$ calcd 536.1193, found 536.1195 [M+H]$^+$.

5.6. General procedure for the preparation of 10a–c

To the solution of **9a–c** (1.5 mmol) in CH_3CN (15 mL) were added 60% NaH (120 mg, 3.0 mmol). The mixture was stirred for 3 h at 80 °C. Then, water (10 mL) was added, and the mixture was concentrated by rotary evaporation. Additional water was added and extracted with EtOAc, and the organic layer was washed with brine, dried with anhydrous sodium sulfate, filtered and evaporated in vacuum to give the corresponding title compounds **10a–c**, which were carried onto the next step without further purification.

5.7. General procedure for the preparation of 11a–c

To the solution of **6** (100 mg, 0.26 mmol) and **10a–c** (0.31 mmol) in ethanol (15 mL) were added L-proline (12 mg, 0.1 mmol). The mixture was stirred for 10 h at rt. After the completion of reaction, the mixture was evaporated under reduced pressure and the residue was purified by column chromatography (PE/EtOAc = 15:1–5:1) to yield the title compounds, respectively.

5.7.1. (*E*)-Methyl 5′-(2-cyano-3-(4-methoxyphenyl)-3-oxoprop-1-en-1-yl)-7,7′-dimethoxy-{4,4′-bibenzo[*d*][1,3]dioxole}-5-carboxylate (11a)

The title compound was obtained starting from **6** and **10a**. As a yellow solid, yield: 87%; mp: 76–78 °C. Analytical data for **11a**: ^{1}H NMR ($CDCl_3$, 300 MHz, δ ppm): 3.69 (s, 3H, OCH_3), 3.87 (s, 3H, OCH_3), 3.97 (s, 3H, OCH_3), 4.03 (s, 3H, OCH_3), 5.92–6.08 (m, 4H, 2 × OCH_2O), 6.89 (d, 2H, 2 × Ar-H, J = 8.4 Hz), 7.36 (s, 1H, Ar-H), 7.73 (s, 2H, 2 × Ar-H), 7.76 (s, 1H, Ar-H), 7.98 (s, 1H, C*H*=CCN); ^{13}C NMR ($CDCl_3$, 75 MHz, δ ppm): δ 21.6 (CH_3), 52.2 (COO*C*H_3), 55.5 (OCH_3), 56.6 (OCH_3), 56.7 (OCH_3), 102.3 (2 × OCH_2O), 108.2, 108.7 (CH=*C*HCO), 109.7 (CN), 112.1, 113.7 (2 × ArC), 114.3, 117.6, 124.4, 125.1, 128.5, 131.6 (2 × ArC), 132.3, 138.4, 139.0, 143.3, 143.4, 143.8, 147.1, 147.9, 152.6 (*C*H=CHCO), 163.6, 165.9 (**C**OOCH$_3$), 187.8 (CH=CH*C*O); IR (KBr, cm^{-1}): ν 2914, 2365, 1714, 1637, 1602, 1410, 1384, 1354, 1254, 1174, 1101, 1039, 924, 750; ESI-MS: m/z 546 [M+H]$^+$, 568 [M+Na]$^+$; HRMS (ESI m/z) for $C_{29}H_{24}NO_{10}$ calcd 546.1400, found 546.1403 [M+H]$^+$.

5.7.2. (*E*)-Methyl 5′-(2-cyano-3-oxo-3-(*p*-tolyl)prop-1-en-1-yl)-7,7′-dimethoxy-{4,4′-bibenzo[*d*][1,3]dioxole}-5-carboxylate (11b)

The title compound was obtained starting from **6** and **10b**. As a yellow solid, yield: 88%; mp: 133–135 °C. Analytical data for **11b**: ^{1}H NMR ($CDCl_3$, 300 MHz, δ ppm): 2.41 (s, 3H, CH_3), 3.69 (s, 3H, OCH_3), 3.98 (s, 3H, OCH_3), 4.04 (s, 3H, OCH_3), 5.92–6.08 (m, 4H, 2 × OCH_2O), 7.20 (d, 2H, 2 × Ar-H, J = 8.0 Hz), 7.36 (s, 1H, Ar-H), 7.60 (d, 2H, 2 × Ar-H, J = 8.0 Hz). 7.67 (s, 1H, Ar-H), 8.01 (s, 1H, C*H*=CCN); ^{13}C NMR ($CDCl_3$, 75 MHz, δ ppm): δ 21.6 (CH_3), 52.1 (COO*C*H_3), 56.6 (OCH_3), 56.7 (OCH_3), 102.5 (OCH_2O), 102.6 (OCH_2O), 108.4, 108.7 (CH=*C*HCO), 108.8 (CN), 112.1, 114.4, 117.4, 124.4, 125.0, 129.0 (2 × ArC), 129.1 (2 × ArC), 133.4, 138.4, 139.1, 143.3, 143.4, 143.8, 147.1, 147.8, 153.1 (*C*H=CHCO), 165.9 (*C*OOCH$_3$), 189.2 (CH=CH*C*O); IR (KBr, cm^{-1}): ν 2946, 1715, 1637, 1604, 1576, 1466, 1433, 1327, 1268, 1245, 1174, 1097, 1062, 1041, 930, 832, 751; ESI-MS: m/z 530 [M+H]$^+$, 552 [M+Na]$^+$; HRMS (ESI m/z) for $C_{29}H_{24}NO_9$ calcd 530.1451, found 530.1453 [M+H]$^+$.

5.7.3. (*E*)-Methyl 5′-(2-cyano-3-oxo-3-(3,4,5-trimethoxyphenyl)prop-1-en-1-yl)-7,7′-dimethoxy-{4,4′-bibenzo[*d*][1,3]dioxole}-5-carboxylate (11c)

The title compound was obtained starting from **6** and **10c**. As a yellow solid, yield: 35%; mp: 82–84 °C. Analytical data for **11c**: ^{1}H NMR ($CDCl_3$, 300 MHz, δ ppm): 3.69 (s, 3H, OCH_3), 3.87 (s, 6H, 2 × OCH_3), 3.92 (s, 3H, OCH_3), 3.97 (s, 3H, OCH_3), 4.04 (s, 3H, OCH_3), 5.92–6.05 (m, 4H, 2 × OCH_2O), 7.08 (s, 2H, 2 × Ar-H), 7.36 (s, 1H, Ar-H), 7.90 (s, 1H, Ar-H), 8.06 (s, 1H, C*H*=CCN); ^{13}C NMR ($CDCl_3$, 75 MHz, δ ppm): δ 52.1 (COO**C**H_3), 56.4 (2 × OCH_3), 56.6 (OCH_3), 56.7 (OCH_3), 61.0 (OCH_3), 102.5 (OCH_2O), 102.6 (OCH_2O), 107.0 (2 × ArC), 107.6 (CH=*C*HCO), 107.7 (CN), 108.5, 112.1,112.2, 118.0, 124.4, 124.9, 130.9, 138.4, 139.4, 143.3, 143.4, 143.8, 147.1,

147.8, 153.0 (CH=CHCO), 153.6 (2 × ArC), 165.9 ($COOCH_3$), 187.7 (CH=CHCO); IR (KBr, cm^{-1}): *v* 2942, 2371, 1718, 1636, 1583, 1415, 1384, 1356, 1331, 1174, 1127, 1102, 1036, 930, 755; ESI-MS: *m/z* 606 $[M+H]^+$, 628 $[M+Na]^+$; HRMS (ESI *m/z*) for $C_{31}H_{28}NO_{12}$ calcd 606.1612, found 606.1615 $[M+H]^+$.

5.8. Biological assays

5.8.1. Cytotoxicity assay

1×10^4 K562 and K562/A02 cells were grown in 96-well microtiter plates and incubated for 24 h. Various concentrations of compounds diluted with medium were added into the wells. And the exponentially growing cancer cells were incubated for 72 h at 37 °C (5% CO_2, 95% humidity). Then, MTS was added directly to the cells. After additional incubation for 3 h at 37 °C, the absorbance at 490 nm was read on a microplate reader (Thermo, USA). The IC_{50} values of the compounds for cytotoxicity were calculated by GraphPad Prism 3.0 software from the dose–response curves.

5.8.2. Flow cytometric analysis

1×10^6 K562/A02 or K562 cells in culture were pre-incubated with different concentrations of the target compounds, VRP or vehicle control (0.1% DMSO) at 37 °C for 1 h, followed by addition of 0.5 μM Rh123 and incubation for 30 min, respectively. Then, the cells were washed with ice-cold PBS three times, and analysis by flow cytometry.

5.8.3. Duration of chemo-sensitizing effect of 8g

1×10^5 cells were plated in 96-well plates and cultured overnight, followed by incubation with 10 μM **8g** or VRP for 24 h. Then, the cells were washed with PBS three times and resuspended in fresh medium. Various concentrations of ADR was added to the culture at the time points (0, 6, 12, and 24 h) after removal of **8g** or VRP, and the cells were incubated for an additional 72 h (5% CO_2, 95% humidity). MTS was added and absorbance at 490 nm was read on a microplate reader (Thermo, USA). The IC_{50} values of the compounds for cytotoxicity were calculated by GraphPad Prism 3.0 software from the dose–response curves.

5.8.4. Western blot analysis

K562/A02 cells were incubated with 10 μM individual compound or vehicle control for 48 h, respectively. And then, the cells were harvested and lyzed. The cell lysates (30 μg) were separated by SDS–PAGE (12% gel) and transferred onto a PVDF membrane. After blocked in a solution containing 5% non-fat milk in TBST buffer, the target proteins were probed with anti-P-gp, anti-GAPDH antibody, respectively. Subsequently, the membranes were washed twice with TBST buffer and incubated with horseradish peroxidase-conjugated secondary antibody. After additional washes with TBST buffer, the protein-antibody complex were visualized by the enhanced Phototope TM-HRP Detection Kit (Cell Signaling, USA) and exposed to Kodak medical X-ray processor (Kodak, USA).

5.8.5. RT-PCR analysis

K562/A02 cells were seeded in 6-well plates at a density of 5×10^5 cells and then cultured without or with 10 μM target compounds for 48 h. Total RNA was extracted and then reverse transcripted from mRNA to cDNA using the RT-PCR kit (Promega, WI, USA). The PCR profile was as follows: 10 min at 95 °C, followed by 30 cycles of 30 s at 95 °C and 1 min at 60 °C. The standard curve and data analysis were produced using Bio-Rad iQ5 software. The relative mRNA level treated with inhibitors was expressed as fold change of the control (in the presence of 0.1% DMSO).

5.8.6. P-gp ATPase assay

Drug-stimulated activity of P-gp ATPase was detected by P-gp-Glo™ assay system (Promega, USA). By following the user protocol provided by the vender, the activity of P-gp ATPase was measured in the presence or absence of 200 μM Na_3VO_4, 200 μM VRP (as a positive reference), 40 μM **8g**. The luminescence was detected in a luminometer (Perkin–Elmer TD-20, USA).

Acknowledgments

The work was financially supported by the Innovative Program for Postgraduate Students of Jiangsu province (NO. CX10B-372Z) and National Natural Science Foundation of China Grant No. 30873083 and 81173082, respectively. We thank to Professor Dongsheng Xiong (Institute of Hematology & Blood Diseases Hospital, CAMS & PUMC, China) for providing K562 and K562/A02 cell lines.

References and notes

1. Aller, S. G.; Yu, J.; Ward, A.; Weng, Y.; Chittaboina, S.; Zhuo, R.; Harrell, P. M.; Trinh, Y. T.; Zhang, Q.; Urbatsch, I. L.; Chang, G. *Science* **2009**, *323*, 1718.
2. Turk, D.; Hall, M. D.; Chu, B. F.; Ludwig, J. A.; Fales, H. M.; Gottesman, M. M.; Szakacs, G. *Cancer Res.* **2009**, *69*, 8293.
3. Martelli, C.; Alderighi, D.; Coronnello, M.; Dei, S.; Frosini, M.; Le Bozec, B. N. D.; Manetti, D.; Neri, A.; Romanelli, M. N.; Salerno, M.; Scapecchi, S.; Mini, E.; Sgaragli, G.; Teodori, E. *J. Med. Chem.* **2009**, *52*, 807.
4. Fletcher, J. I.; Haber, M.; Henderson, M. J.; Norris, M. D. *Nat. Rev. Cancer* **2010**, *10*, 147.
5. Zhang, L.; Ma, S. *ChemMedChem* **2010**, *5*, 811.
6. Colabufo, N. A.; Berardi, F.; Cantore, M.; Contino, M.; Inglese, C.; Niso, M.; Perrone, R. *J. Med. Chem.* **1883**, *2010*, 53.
7. Wu, C. P.; Ohnuma, S.; Ambudkar, S. V. *Curr. Pharm. Biotechnol.* **2011**, *12*, 609.
8. Crowley, E.; McDevitt, C. A.; Callaghan, R. *Methods Mol. Biol.* **2010**, *596*, 405.
9. Aponte, J. C.; Verástegui, M.; Málaga, E.; Zimic, M.; Quiliano, M.; Vaisberg, A. J.; Gilman, R. H.; Hammond, G. B. *J. Med. Chem.* **2008**, *51*, 6230.
10. Liu, X. L.; Tee, H. W.; Go, M. L. *Bioorg. Med. Chem.* **2008**, *16*, 171.
11. Tang, X.; Gu, X.; Ai, H.; Wang, G.; Peng, H.; Lai, Y.; Zhang, Y. *Bioorg. Med. Chem. Lett.* **2012**, *22*, 801.
12. Chang, J.; Chen, R.; Guo, R.; Dong, C.; Zhao, K. *Helv. Chim. Acta* **2003**, *86*, 2239.
13. Tatsuzaki, J.; Bastow, K. F.; Nakagawa-Goto, K.; Nakamura, S.; Itokawa, H.; Lee, K. H. *J. Nat. Prod.* **2006**, *69*, 1445.
14. Baumert, C.; Hilgeroth, A. *Anticancer Agents Med. Chem.* **2009**, *9*, 415.
15. Teodori, E.; Dei, S.; Quidu, P.; Budriesi, R.; Chiarini, A.; Garnier-Suillerot, A.; Gualtieri, F.; Manetti, D.; Romanelli, M. N.; Scapecchi, S. *J. Med. Chem.* **1999**, *42*, 1687.
16. Kong, X. W.; Zhang, Y. H.; Wang, T.; Lai, Y. S.; Peng, S. X. *Chem. Biodivers.* **2008**, *5*, 1743.
17. Ma, Y.; Wink, M. *Phytomedicine* **2008**, *15*, 754.
18. Yang, C. Z.; Luan, F. J.; Xiong, D. S.; Liu, B. R.; Xu, Y. F.; Gu, K. S. *Zhongguo Yao Li Xue Bao* **1995**, *16*, 333.
19. Jin, J.; Sun, H.; Wei, H.; Liu, G. *Invest. New Drugs* **2007**, *25*, 95.
20. Qi, J.; Wang, S.; Liu, G.; Peng, H.; Wang, J.; Zhu, Z.; Yang, C. *Biochem. Biophys. Res. Commun.* **2004**, *319*, 1124.
21. Dai, C. L.; Tiwari, A. K.; Wu, C. P.; Su, X. D.; Wang, S. R.; Liu, D. G.; Ashby, C. R., Jr.; Huang, Y.; Robey, R. W.; Liang, Y. J.; Chen, L. M.; Shi, C. J.; Ambudkar, S. V.; Chen, Z. S.; Fu, L. W. *Cancer Res.* **2008**, *68*, 7905.
22. Martelli, C.; Alderighi, D.; Coronnello, M.; Dei, S.; Frosini, M.; Le Bozec, B.; Manetti, D.; Neri, A.; Romanelli, M. N.; Salerno, M.; Scapecchi, S.; Mini, E.; Sgaragli, G.; Teodori, E. *J. Med. Chem.* **2009**, *52*, 807.
23. Krawczyk, S.; Otto, M.; Otto, A.; Coburger, C.; Krug, M.; Seifert, M.; Tell, V.; Molnar, J.; Hilgeroth, A. *Bioorg. Med. Chem.* **2011**, *19*, 6309.
24. Wang, Y. M.; Hu, L. X.; Liu, Z. M.; You, X. F.; Zhang, S. H.; Qu, J. R.; Li, Z. R.; Li, Y.; Kong, W. J.; He, H. W.; Shao, R. G.; Zhang, L. R.; Peng, Z. G.; Boykin, D. W.; Jiang, J. D. *Clin. Cancer Res.* **2008**, *14*, 6218.